Sliding Mode Control of a Variable Speed Wind Energy Conversion System based on DFIG

Nihel Khemiri[1], Adel Khedher[2,4], Mohamed Faouzi Mimouni[3,1]

[1]Research unit ESIER, Monastir, Tunisia. khemirin@yahoo.fr
[2]National Engineering School of Sousse ENISo, Sousse, Tunisia. Adel_kheder@yahoo.fr
[3]National Engineering School of Monastir ENIM, Monastir, Tunisia. Mfmimouni@enim.rnu.tn
[4]Research unit RELEV, ENIS, Sfax, Tunisia.

Abstract: *This article is devoted to the study of the performances of nonlinear sliding mode control (SMC) of a variable speed wind energy conversion system (WECS) based on a doubly Fed Induction Generator (DFIG). The SMC strategy is applied to both Rotor Side Converter (RSC) and Grid Side Converter (GSC). The RSC controls the active and reactive powers produced by the DFIG. The GSC controls the DC-bus voltage and the power factor. Simulations results show interesting performances of the system in terms of the robustness against parameters variations.*

Key Words: *Double fed induction generator, sliding mode control, rotor side converter, grid side converter.*

1. Introduction

The evolution of technology related to wind systems industry leaded to the development of a generation of variable speed wind turbines. These wind energy conversion systems are connected to the grid through voltage source converters (VSC) to make variable speed operation possible. The WECS using a doubly-fed induction generator (DFIG) have some advantages due to variable speed operation and four quadrants active and reactive power capabilities compared with fixed speed induction generators.

There are many different control schemes of DFIG, generally based on vector control concept considering stator flux or voltage orientation principle associated with PI, back-to-back controllers [1]. The aim of this paper is to apply a sliding mode control (SMC). The use of this control mode can be justified by the high performances required by DFIG and the robustness of the controller.

The stator active and reactive powers are regulated by controlling the rotor current vector using field oriented control (FOC), based on linear PI controllers, have so far proved to be the most popular control technique, although it is clear that its drawbacks are its linear nature and lack of robustness when faced with changes in operational conditions [2].

The SMC is nowadays frequently used because of its simplicity and efficiency, it is not sensible to parameters variations and external disturbances [3]. This paper proposes to apply the SMC to a DFIG used in wind-energy conversion systems. The DFIG consists of a wound rotor induction generator directly connected to the grid through two power converters: Rotor Side Converter (RSC) and Grid Side Converter (GSC).

The RSC controls the active and reactive powers produced by the machine. The grid-side converter is usually used to regulate the DC-bus voltage between the two converters regardless of the magnitude and direction of the rotor power, while keeping sinusoidal grid currents. The basic configuration of the whole system is presented in Figure 1.

This paper is organized as follows: In second section, we have presented a mathematical model of DFIG. The third section is devoted to study the design of sliding mode control algorithm. We have presented in the first step the RSC control under SMC and the GSC control in the second step. In the last section, some simulation results are shown interesting obtained control performances of the DFIG in terms of the reference tracking ability and the robustness against parameters variations.

2. Mathematical model of a DFIG

Under the assumption of linear magnetic circuits and balanced operating conditions, the equivalent two-

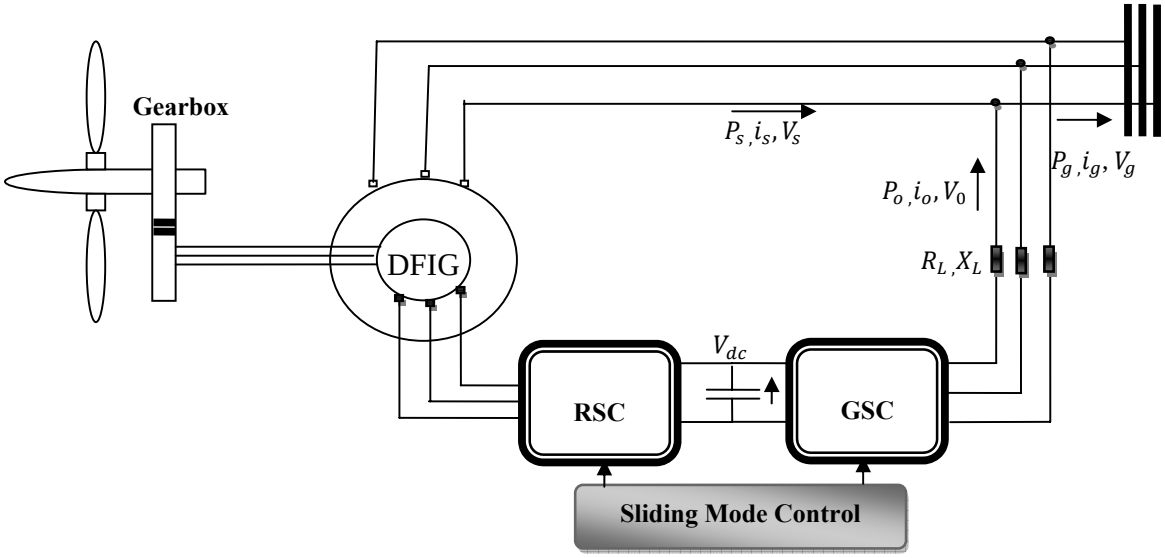

Fig .1. WECS-based DFIG topology.

phase model of the symmetrical DFIG, represented in *dq* reference frame is as follows [4]:

$$\begin{cases} V_{sd} = R_s i_{sd} + \frac{d\Phi_{sd}}{dt} - \Phi_{sq}\omega_s \\ V_{sq} = R_s i_{sq} + \frac{d\Phi_{sq}}{dt} + \Phi_{sd}\omega_s \\ V_{rd} = R_r i_{rd} + \frac{d\Phi_{rd}}{dt} - \Phi_{rq}\omega_r \\ V_{rq} = R_s i_{rq} + \frac{d\Phi_{rq}}{dt} + \Phi_{rd}\omega_r \end{cases} \quad (1)$$

The stator and rotor flux can be expressed as [4]:

$$\begin{cases} \Phi_{sd} = L_s i_{sd} + M i_{rd} \\ \Phi_{sq} = L_s i_{sq} + M i_{rq} \\ \Phi_{rd} = L_r i_{rd} + M i_{sd} \\ \Phi_{rq} = L_r i_{rq} + M i_{sq} \end{cases} \quad (2)$$

By choosing a reference frame linked to the stator flux and the stator resistance is neglected, which is a realist approximation for medium and high power machines used in wind energy conversion, the stator voltage vector is consequently in quadrature advance against stator flux [5] and are given by:

$$\begin{cases} V_{sd} = 0 \\ V_{sq} = \omega_s \Phi_{sd} \end{cases} \quad (3)$$

$$\begin{cases} \Phi_{sq} = 0 \\ \Phi_{sd} = \Phi_s \end{cases} \quad (4)$$

The stator active and reactive power can be expressed as follows:

$$\begin{cases} P_s = -\frac{3}{2} V_{sq} \frac{M}{L_s} i_{rq} \\ Q_s = \frac{3}{2}\left(\frac{V_{sq}\Phi_{sd} - V_{sq} M i_{rd}}{L_s}\right) \end{cases} \quad (5)$$

According to Eq.(2) and (4), the stator currents are given by:

$$\begin{cases} i_{sd} = \frac{\Phi_{sd} - M i_{rd}}{L_s} \\ i_{sq} = -\frac{M}{L_s} i_{rq} \end{cases} \quad (6)$$

The rotor fluxs are expressed by:

$$\begin{cases} \Phi_{rd} = \sigma L_r i_{rd} + \frac{M}{L_s}\frac{V_{sq}}{\omega_s} \\ \Phi_{rq} = \sigma L_r i_{rq} + + \frac{M}{L_s}\frac{V_{sd}}{\omega_s} \end{cases} \quad (7)$$

Based on Eq. (7), the rotor current can be expressed as:

$$\begin{cases} i_{rd} = \frac{1}{\sigma L_r}\left(\sigma L_r i_{rd} + \frac{M}{L_s}\frac{V_{sq}}{\omega_s}\right) - \frac{M\Phi_{sd}}{\sigma L_r L_s} \\ i_{rq} = \frac{1}{\sigma L_r}\left(\sigma L_r i_{rq} + \frac{M}{L_s}\frac{V_{sd}}{\omega_s}\right) - \frac{M\Phi_{sq}}{\sigma L_r L_s} \end{cases} \quad (8)$$

The stator currents are written as follows:

$$\begin{cases} i_{sd} = \frac{(\Phi_{sd}L_r - M\Phi_{rd})}{\sigma L_s L_r} \\ i_{sq} = \frac{(\Phi_{sq}L_r - M\Phi_{rq})}{\sigma L_s L_r} \end{cases} \quad (9)$$

By replacing of fluxs, the stators current are given by:

$$\begin{cases} i_{sd} = \frac{1}{\sigma L_s}\Phi_{sd} - \frac{M}{\sigma L_r L_s}\left(\sigma L_r i_{rd} + \frac{M}{L_s}\frac{V_{sq}}{\omega_s}\right) \\ i_{sq} = \frac{1}{\sigma L_s}\Phi_{sq} - \frac{M}{\sigma L_r L_s}(\sigma L_r i_{rq} + + \frac{M}{L_s}\frac{V_{sd}}{\omega_s}) \end{cases} \quad (10)$$

Accounting for equations (7), (8) and (10), the stator and rotor voltages are given by Eq. (11).

$$\begin{cases} V_{sd} = R_s a\Phi_{sd} - R_s c\left(\sigma L_r i_{rd} + \frac{M}{L_s}\frac{V_{sq}}{\omega_s}\right) + \frac{d\Phi_{sd}}{dt} - \Phi_{sq}\omega_s \\ V_{sq} = R_s a\Phi_{sq} - R_s c\left(\sigma L_r i_{rq} + \frac{M}{L_s}\frac{V_{sd}}{\omega_s}\right) + \frac{d\Phi_{sq}}{dt} + \Phi_{sd}\omega_s \\ V_{rd} = R_r b\left(\sigma L_r i_{rd} + \frac{M}{L_s}\frac{V_{sq}}{\omega_s}\right) + \sigma L_r\frac{di_{rd}}{dt} - \omega_r\left(\sigma L_r i_{rq} + \frac{M}{L_s}\frac{V_{sd}}{\omega_s}\right) \\ \qquad -R_r c\Phi_{sd} \\ V_{rq} = R_r b\left(\sigma L_r i_{rq} + \frac{M}{L_s}\frac{V_{sd}}{\omega_s}\right) + \sigma L_r\frac{di_{rq}}{dt} + \omega_r\left(\sigma L_r i_{rd} + \frac{M}{L_s}\frac{V_{sq}}{\omega_s}\right) \\ \qquad -R_r c\Phi_{sq} \end{cases} \quad (11)$$

With:

$$\sigma = 1 - \frac{M^2}{L_s L_r}\ ;\ a = \frac{1}{\sigma L_s};\ b = \frac{1}{\sigma L_r};\ c = \frac{M}{\sigma L_s L_r}$$

The state model can then be written as [6]:

$$\dot{X} = f(X,t) + g(X,t)U_{dq} \quad (12)$$

$$\dot{X} = \begin{bmatrix} \frac{d\Phi_{sd}}{dt} \\ \frac{d\Phi_{sq}}{dt} \\ \frac{di_{rd}}{dt} \\ \frac{di_{rq}}{dt} \end{bmatrix};\ U_{dq} = \begin{bmatrix} V_{sd} \\ V_{sq} \\ V_{rd} \\ V_{rq} \end{bmatrix}\ ;\ g(X,t) = \begin{bmatrix} 1 & 0 & 0 & 0 \\ 0 & 1 & 0 & 0 \\ 0 & 0 & \frac{1}{\sigma L_r} & 0 \\ 0 & 0 & 0 & \frac{1}{\sigma L_r} \end{bmatrix} \quad (13)$$

With

$$f(X,t) = \begin{bmatrix} -R_s a\Phi_{sd} + R_s c\left(\sigma L_r i_{rd} + \frac{M}{L_s}\frac{V_{sq}}{\omega_s}\right) + \Phi_{sq}\omega_s \\ -R_s a\Phi_{sq} + R_s c\left(\sigma L_r i_{rq} + \frac{M}{L_s}\frac{V_{sd}}{\omega_s}\right) - \Phi_{sd}\omega_s \\ \frac{1}{\sigma L_r}\left(-R_r b\left(\sigma L_r i_{rd} + \frac{M}{L_s}\frac{V_{sq}}{\omega_s}\right) + R_r c\Phi_{sd} + \omega_r\left(\sigma L_r i_{rq} + \frac{M}{L_s}\frac{V_{sd}}{\omega_s}\right)\right) \\ \frac{1}{\sigma L_r}\left(-R_r b\left(\sigma L_r i_{rq} + \frac{M}{L_s}\frac{V_{sd}}{\omega_s}\right) + R_r c\Phi_{sq} - \omega_r\left(\sigma L_r i_{rd} + \frac{M}{L_s}\frac{V_{sq}}{\omega_s}\right)\right) \end{bmatrix} \quad (14)$$

3. Design of sliding mode control algorithm

The method consists to calculate the equivalent and discontinuous components [7] of control variable from an adequate surface of sliding mode chosen [8].

3.1. Rotor side converter control

The rotor currents (which are linked to active and reactive powers by Eq. (5)) have to track appropriate current references, so, a sliding mode control based on the above Park reference frame is used [9].
Sliding surfaces represent the error between the actual and references rotor currents and are expressed as follows:

$$\begin{cases} S_d = i_{rd\_ref} - i_{rd} \\ S_q = i_{rq\_ref} - i_{rq} \end{cases} \quad (15)$$

V_{rd} and V_{rq} will be the two components of the control vector used to constraint the system to converge to $S_{dq} = 0$. The equivalent vector control $U_{eq_{dq}}$ is computed by imposing $\dot{S}_{dq} = 0$ so the equivalent control components are given by the equation (16).

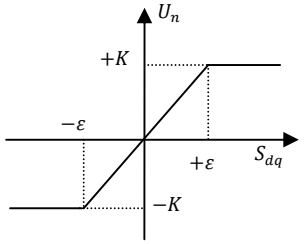

Fig. 2. Smoothed sign function.

$$U_{eq_{dq}} = \begin{bmatrix} -[-R_r b\left(\sigma L_r i_{rd} + \frac{M}{L_s}\frac{V_{sq}}{\omega_s}\right) + R_r c\Phi_{sd} + \omega_r\left(\sigma L_r i_{rq} + \frac{M}{L_s}\frac{V_{sd}}{\omega_s}\right)] \\ -[-R_r b\left(\sigma L_r i_{rq} + \frac{M}{L_s}\frac{V_{sd}}{\omega_s}\right) + R_r c\Phi_{sq} - \omega_r\left(\sigma L_r i_{rd} + \frac{M}{L_s}\frac{V_{sq}}{\omega_s}\right)] \end{bmatrix} \quad (16)$$

However, the equivalent vector control produces a drawback in the performances of a control system, which is known as chattering phenomenon [8]. To reduce the phenomenon, a smooth function is defined in some neighborhood of the sliding surface with a threshold as seen in Figure 2, [10].

To obtain some good performance dynamic the control vector is imposed as follows:

$$U_{dq} = U_{eq_{dq}} + K_{dq} sign(S_{dq}) \quad (17)$$

In order to guarantee the attractiveness of the sliding surface, the nonlinear component is added to the global function of the controller [4].

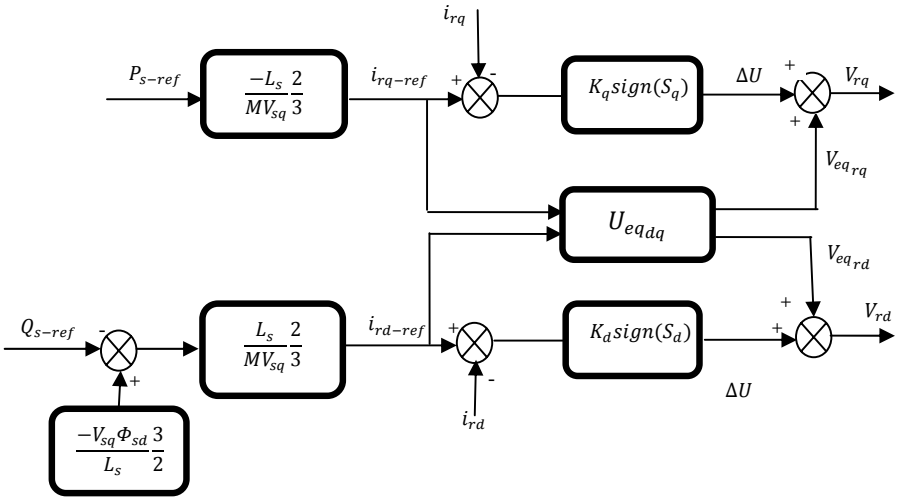

Fig. 3. SMC structure applied to the RSC of WECS based on the DFIG.

3.2. Grid side converter control

The GSC is connected to the electrical grid by an intermediary line characterized by a resistance R_L and a reactance X_L [11]. In a reference Park frame related to the network angular speed $\boldsymbol{\omega_R}$ equal to the synchronous speed, the electrical voltage equation is given by:

$$\begin{cases} \frac{di_{od}}{dt} = \frac{V_{od}}{L} - \frac{R}{L} i_{od} + \omega_R i_{oq} \\ \frac{di_{oq}}{dt} = \frac{V_{oq}}{L} - \frac{R}{L} i_{oq} - \omega_R i_{od} - V_{gd} \end{cases} \quad (18)$$

The active and the reactive power are given by follows [12]:

$$\begin{cases} P_0 = \frac{3}{2}(V_{gd} i_{od} + V_{gq} i_{oq}) \\ Q_0 = \frac{3}{2}(V_{gq} i_{od} - V_{gd} i_{oq}) \end{cases} \quad (19)$$

We present in this part a study on the regulation power. This study is based on network voltage vector oriented control. This method is based on the orientation of grid voltage along Park d-axis. This implies that $V_{gd} = |\overline{V_g}|$ and $V_{gq} = 0$ [13].

In these conditions, one can write [1]:

$$\begin{cases} P_0 = \frac{3}{2} V_{gd} i_{od} \\ Q_0 = -\frac{3}{2} V_{gd} i_{oq} \end{cases} \quad (20)$$

As shown in relations (20) the dynamics of the active and reactive power are directly linked to the control of grid currents i_{od} and i_{oq}. voltage is constant and equal to the nominal AC voltage. For the DFIG sliding mode controllers design, two switching surfaces are chosen as:

$$\begin{cases} S_1 = i_{od\_ref} - i_{od} \\ S_2 = i_{oq\_ref} - i_{oq} \end{cases} \quad (21)$$

In order to converge S to zero in finite time, the control law is designed such as:

$$\begin{bmatrix} \dot{S}_1 \\ \dot{S}_2 \end{bmatrix} = - \begin{bmatrix} K_1 . sign(S_1) \\ K_2 . sign(S_2) \end{bmatrix} \quad (22)$$

By the development of Equation (18) we write:

$$\frac{V_{od}}{L} - \left(\frac{R_L}{L} i_{od_{ref}} - \omega_R i_{oq_{ref}} \right) = -K_1 . sign(S_1) \quad (23)$$

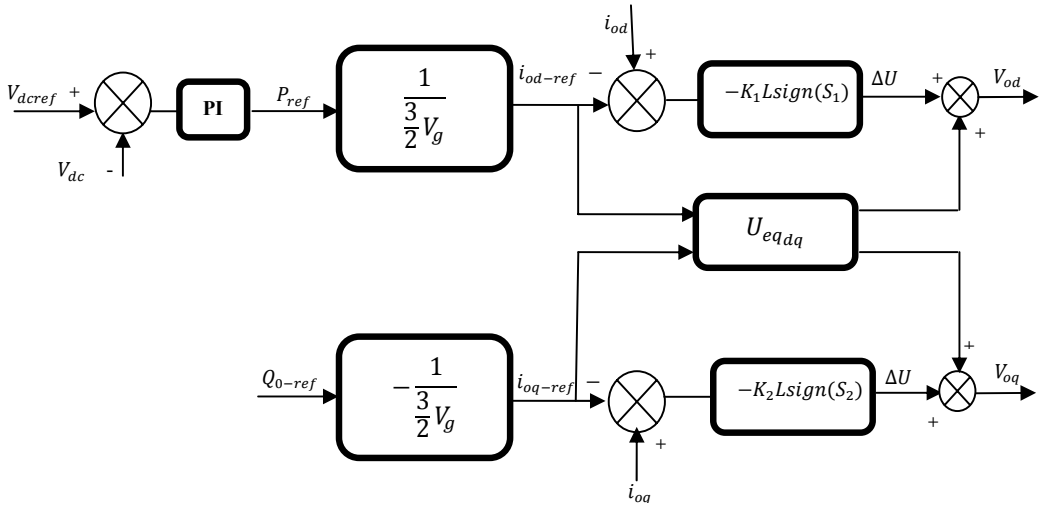

Fig. 4. SMC structure applied to the GSC of WECS based on the DFIG.

The direct GSC output current set value is deduced as:

$$i_{od_{ref}} = \frac{2\,P_{0-ref}}{3\,V_{gd}} \quad (24)$$

By the same manner, we can write:

$$\frac{V_{oq}}{L} - \left(\frac{R_L}{L} i_{oq_{ref}} + \omega_R i_{od_{ref}} + \frac{V_{gd}}{L}\right) = K_2.sign(S_2) \quad (25)$$

The quadrature GSC output current set value is deduced as:

$$i_{oq_{ref}} = -\frac{2\,Q_{0-ref}}{3\,V_{gd}} \quad (26)$$

By considering equations (23) on (25) the expression of voltage as follows:

$$\begin{cases} V_{od} = -K_1.L.sign(S_1) + R_L i_{od_{ref}} - \omega_R L\, i_{oq_{ref}} \\ V_{oq} = -K_2.L.sign(S_2) + R_L i_{oq_{ref}} + \omega_R L\, i_{od_{ref}} + V_{gd} \end{cases} \quad (27)$$

With

$$U_{eq_{dq}} = \begin{bmatrix} R_L i_{od_{ref}} - \omega_R L\, i_{oq_{ref}} \\ R_L i_{oq_{ref}} + \omega_R L\, i_{od_{ref}} + V_{gd} \end{bmatrix} \quad (28)$$

4. Simulations results

Simulations results are made by using the real parameters of a wind turbine AE43 and a DFIG rated at 660KW and 690V. The characteristics of this system are given in appendix. In our simulation, the wind profile is governed by the following equation:

$$\begin{cases} V_{wind} = 4 + 6t & t < 1 \\ V_{wind} = 10 & t \geq 1 \end{cases} \quad (29)$$

To studied the comportment of the WECS based on the DFIG against the parameters variations. We have illustrated some simulations scenarios attached to: Stator active power, stator reactive power, rotor resistance and mutual inductance. In all figures we illustrate in (b),(c),(d) and (e) the variation of real stator active power, stator reactive power, the balanced three phase stator currents and the balanced three phase rotor currents. In all figures (a) we illustrate the reference parameters variations.

1. Figure 5 illustrates the response of the WECS based on the DFIG operated under SMC without parameter variations.

2. Figure 6 illustrates the response of the WECS based on the DFIG operated under SMC with reference-stator active power variations.

3. Figure 7 illustrates the response of the WECS based on the DFIG operated under SMC with reference-stator reactive power variations.

4. Figure 8 illustrates the response of the WECS based on the DFIG operated under SMC with reference-rotor resistance variations.

5. Figure 9 illustrates the response of the WECS based on the DFIG operated under SMC with reference-mutual inductance variations.

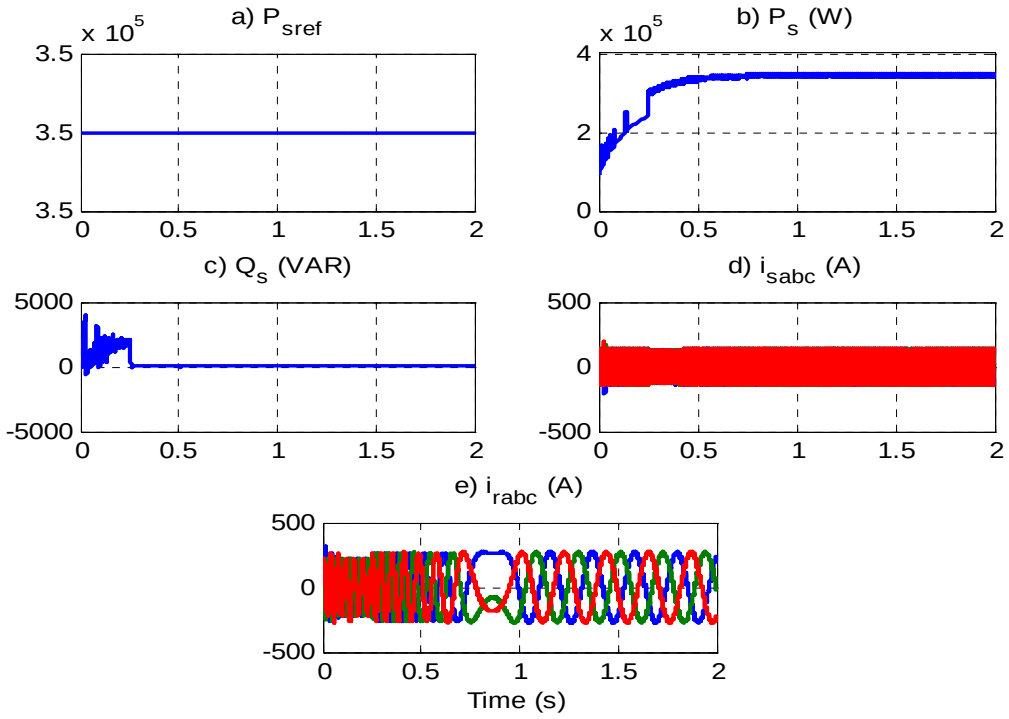

Fig. 5. DFIG operated under SMC strategy without parameter variation:
Legend: (a) P_{sref}, (b) P_s, (c) Q_s, (d) i_{sabc} (e) i_{rabc}

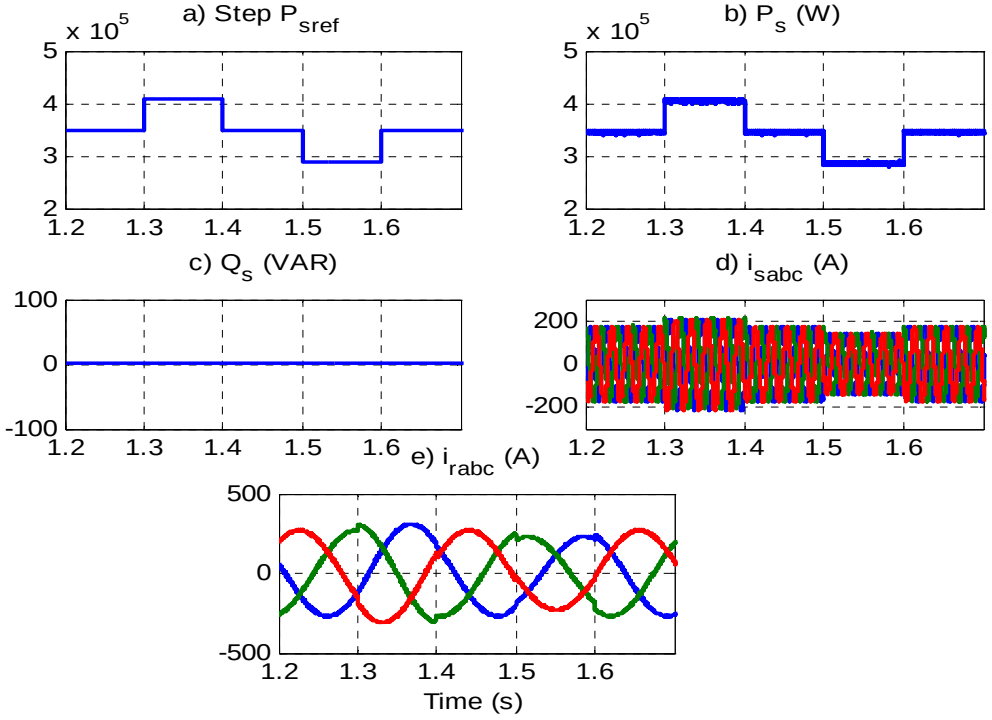

Fig. 6. DFIG operated under SMC strategy with reference active stator power variation:
Legend: (a) P_{sref}, (b) P_s, (c) Q_s, (d) i_{sabc} (e) i_{rabc}

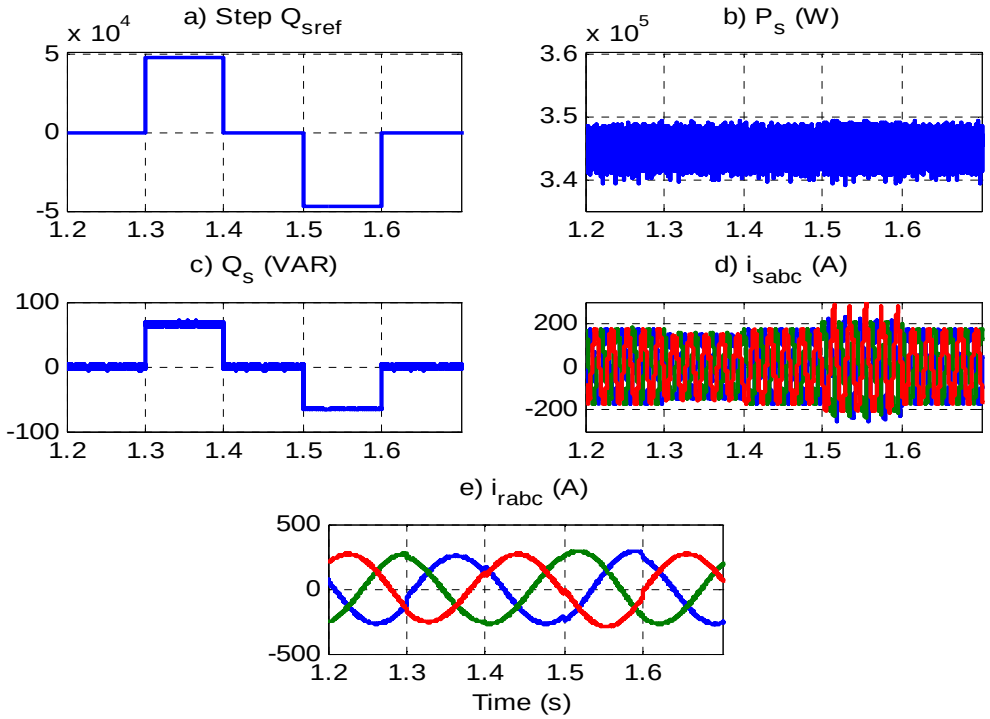

Fig. 7. DFIG operated under SMC strategy with reference reactive stator power variation: Legend: (a) Q_{sref}, (b) P_s, (c) Q_s, (d) i_{sabc} (e) i_{rabc}

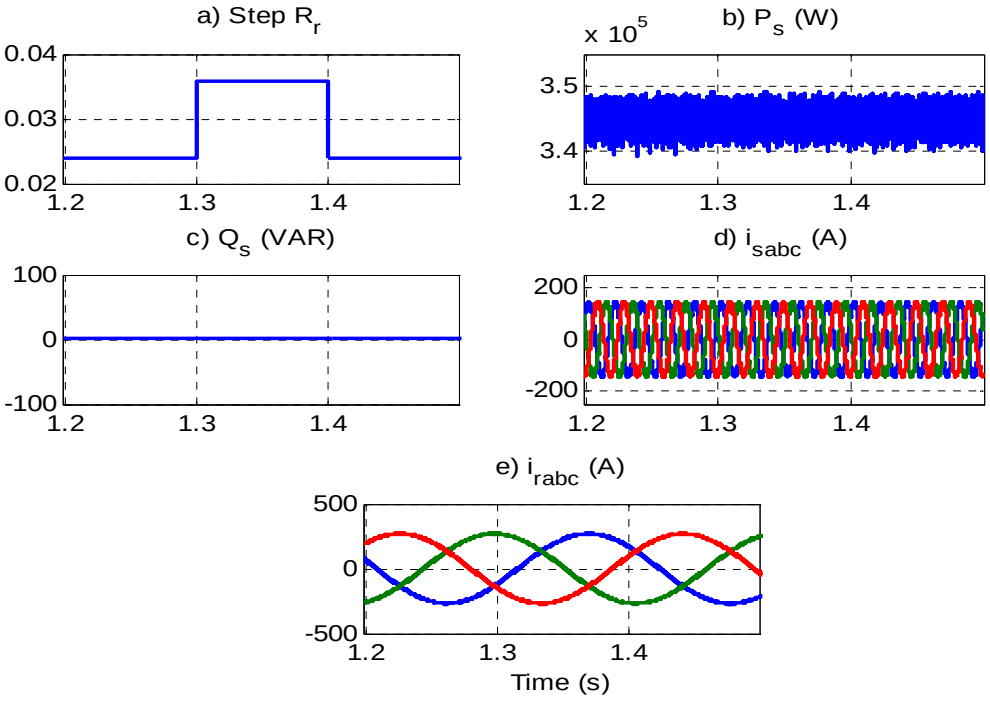

Fig. 8. DFIG operated under SMC strategy with rotor resistance variation: Legend: (a) R_{rref}, (b) P_s, (c) Q_s, (d) i_{sabc} (e) i_{rabc}

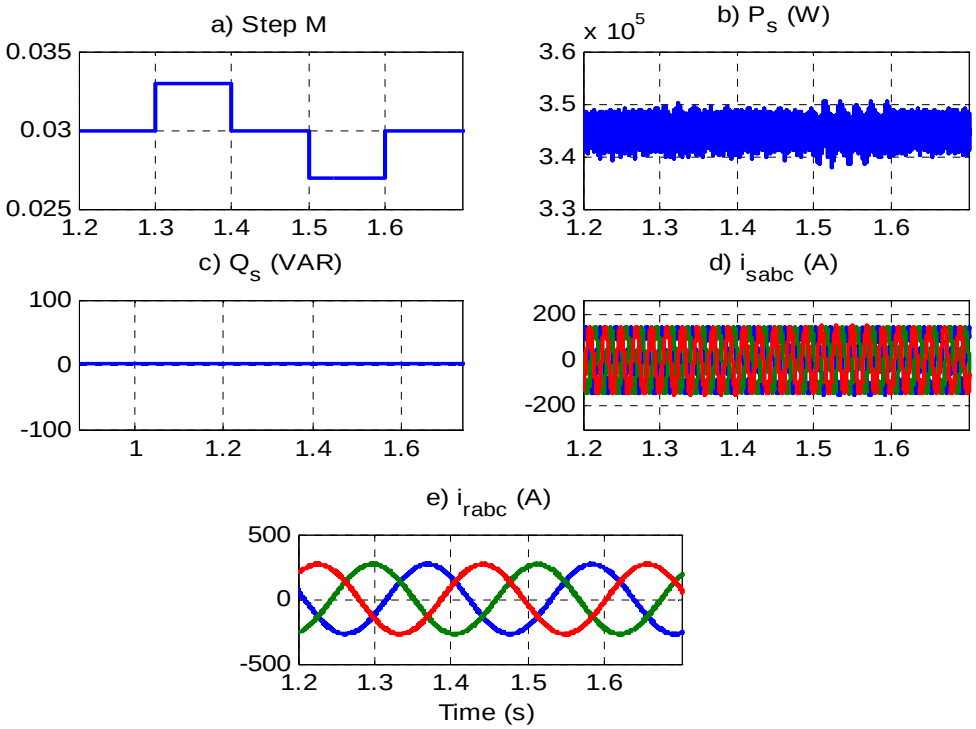

Fig. 9. DFIG operated under SMC strategy with mutual inductance variation:
Legend: (a) M_{ref}, (b) P_s, (c) Q_s, (d) i_{sabc} (e) i_{rabc}

According the illustrations we can remark:

- The step change of one control variable, i.e., stator active or reactive power, does not affect the other.
- We can see that the actual stator active power and stator reactive power follows well the variations of its reference.
- The variation of the reference of stator active power at t=1.3s undergoes an increase of 23% of the stator current and a diminution of same percentage at t=1.5s. Also, it undergoes a variation of ±15% of the rotor current.
- The variation of the reference of stator reactive power at t=1.3s undergoes a decrease of 13% of the stator current and an increase of 35% at t=1.5s. Also, it undergoes a decrease of 4.8% of the rotor current and an increase of 7.5% at t=1.5s.
- Looking at figure 5, we see that the system is efficient when it operates without parameters variations.
- Figures 6 and 7 showed the satisfactory performances of the WECS against, respectively, the variation of reference of the stator active and reactive power.
- Figures 8 and 9 showed the satisfactory performances respectively of the rotor resistance and the magnetizing inductance.

5. Conclusion

This work describes a control approach applied to the WECS based on the DFIG used to extract and transit the maximum power from the wind will to the electrical grid. The system uses two rotor power converters linked by a DC voltage which allow the power energy transient between the grid and the WECS. We have applied the SMC of the DFIG in the both RSC and GSC. This structure has been used for reference tracking of stator active and reactive powers exchanged between the stator and the grid by controlling the rotor converter. The simulations results show that the robustness of the proposed SMC against parameters variations.

References

1. Ben Alaya J., Khedher A., Mimouni M. F.: *DTC, DPC and Nonlinear Vector Control Strategies Applied to the DFIG operated at Variable Speed*. Journal of Electrical Engineering JEE, 2011, Vol. 6, N° 11, pp. 744-753.
2. Serhoud H., Benattous D.: *Sensorless Sliding Power Control of Doubly Fed Induction Wind Generator Based on MRAS Observer*. World Academy of Science, Engineering and Technology , 2011.
3. Machmoum M., Poitiers F.: *Sliding Mode Control of a Variable speed Wind Energy conversion System with DFIG*. Conference on Ecologic Vehicles and Renewable Energy (EVER'09), Monaco, France, March 2009.
4. Naamane A., Msirdi N.K. : *Doubly Feed Induction Generator Control For An Urban Wind Turbine*. International Renewable Energy Congress IREC, pp. 208-214, November 2010.
5. Belmokhtar K., Doumbia M.L., Agbossou K. : *Modelling and Power Control of Wind Turbine Driving DFIG connected to the Utility Grid.* International Conference on Renewable Energies and Power Quality ICREPQ, April 2011.
6. Ouari K., Rekioua T., Ouhrouche M.: *A Non Lineare Predictive Controller For Wind Energy Conversion System.* International Renewable Energy Congress IREC, pp. 220-226, November 2010.
7. Khedher A., Mimouni M.F., Derbel N., Masmoudi A. : *A survey on modeling, estimation and on-line adaptation of induction motor parameters under R.F.O.C.* Trans. on Systems, Signals and Devices, Vol.2, N° 2, pp.177–95, 2007.
8. BekakraY., Ben Attous D. : *Sliding Mode Controls of Active and Reactive Power of a DFIG with MPPT for Variable Speed Wind Energy Conversion.* Australian Journal of Basic and Applied Sciences, December 2011, pp. 2274-2286.
9. Kechich A., Mazari B., Bousserhane K.: *Application of Nonlinear Sliding-Mode Control to Permanent Magnet Synchronous Machine.* International Journal of Applied Engineering Research, 2007, Vol. 2, N° 1, pp. 125-138.
10. Dendouga A., Abdessemed R., Bendaas M.L., Chaiba A.: *Sliding Mode Control of Active and Reactive Powers Generated by a Doubly-Fed Induction Generator (DFIG).* Damascus University Journal, April 2008, Vol. 24.
11. Ben Alaya J., Khedher A., Mimouni M.F. : *Variable Speed Vector Control Strategy of the Double Fed Induction Generator Integrated in Electrical Grid.* Third International Conference on Ecological Vehicles & Renewable Energies (EVER'08), March 2008.
12. Hu J., Nian H., Zhu Z.Q.: *Direct Active and Reactive Power Regulation of DFIG Using Sliding-Mode Control Approach*. IEEE Transactions On Energy Conversion, December 2010,Vol. 25, N° 4.
13. Ben Alaya J., Khedher A., Mimouni M. F. : *DTC and Nonlinear Vector Control Strategies Applied to the DFIG operated at Variable Speed.* WSEAS Transactions on environment and development. 210, Vol. 6, N° 11, pp. 744-753.

Appendix

Induction generator data

Rated power	660Kw
Rated stator voltage	400/690V
Nominal frequency	50 Hz
Number of pole pairs	n_p=2
Rotor resistance	$R_r = 0.0238\Omega$
Stator resistance	$R_s = 0.0146\Omega$
Stator inductance	$L_s = 0.0306H$
Rotor inductance	$L_r = 0.0303$
Mutual inductance	M=0.0299H

Wind turbine data

Rated power	660Kw
Blade Radius	R = 21.165 m
Power coefficient	C_{pmax} = 0.42
Optimal relative wind speed	λ_{opt}= 9
Mechanical speed multiplier	G=39
Moment of inertia	J=28 Kg.m^2
Damping coefficient	f= 0.01